The Polar Express: Investigating the impact of aerosol transport to the poles by Atmospheric Rivers

December 14, 2022

By **Julia Asplund** (julia.asplund@aces.su.se), in collaboration with Lea Haberstock

This study is a part of the project **polARosol- For a brighter future?**: POLar Atmospheric Rivers and how they are influenced by AeROSOLs and how that might affect cloud BRIGHTness but mostly other parameters now and in the FUTURE

Course: **eScience Tools in Climate Science: Linking Observations with Modelling**

Project assistant, fearless leader, person we would not have managed without: Remy Lapere

Abstract

Atomspheric rivers (AR), long atmospheric filaments of enhanced poleward integrated vapour transport, are responsible for 90% of the transportation of moisture from the tropics to mid latitudes. In polar regions they are more rare events, but potentially key drivers of major ice melt events. Not only is the incoming moist air usually warmer than polar surface temperature, further heat is can be added by the triggering of extreme precipitation events, or by increased downwelling longwave radiation due to altered cloud properties. AR can also transport pollution in the form of aerosol particles to the poles, that can further effect cloud parameters such as droplet number concentration and result in a positive or negative feedback effect on the temperature. In this work, AR are detected by applying a detection scheme inspired by Wille et al (2021) to NorESM2 model output from the Historical CMIP6 experiment between 1990 and 2015. Cloud fraction, precipitation rate, surface temperature and downwelling longwave radiation is compared between AR with high and low AOD in the polar regions. The strongest impact is found for surface temperature and longwave radiation, particularly in the Arctic winter where AR with higher AOD are associated with higher values. More studies are needed to determine the cause of this effect, if it due to aerosol transport by AR, or just because of a difference in AOD or latitude. A strong seasonal trend with increased AR occurence is found for the Arctic but not the Antarctic. This study highlights the complexity of AR detection, as issues with detected rivers being too wide and reach the poles arise. Some improvements could be made by making the detection seasonally dependent and using data with higher time resolution, but a discussion on an objective standardized method of AR detection and definition is encouraged.

Introduction

Atmospheric rivers (AR) are long, narrow regions of significantly enhanced poleward moisture transport in the atmosphere. They mostly occur by interactions between large scale atmospheric circulation processes like the hadley cell or low level jets, and are by far the dominant process for poleward transport of moisture from the tropics to the midlatitudes. AR are therefore crucial for precipitation and water security in populated regions. However, they also result in destructive precipation events, causing floods or landslides (Nash et al., 2018, Payne et al., 2020). In the polar regions, AR are relatively rare events since they transport heat along with the moisture and can trigger extreme precipitation events, they still play a significant role in driving sea ice melt, ice sheet calving and changes in precipitation patterns (Nash et al., 2018, Wille et al., 2019). There are still very few studies on AR and their impact polar climate, even though the interest is increasing with the urgency of understanding major climate feedbacks and tipping points for societal resilience against climate change.

The melting of the Greenland Ice Sheet has been shown to be largely driven by a combination of warm air and moisture transport by AR, particularly in summer, and the presence of thin clouds that trap longwave radiation, heating the surface (Neff, 2018). One of the factors affecting the radiative properties of Arctic clouds is aerosols, as aerosol particles acting as cloud condensation nuclei (CCN) are necessary to form cloud droplets. In both polar regions, aerosol particle concentrations are typically several orders of magnitude lower than at mid latitues, which means there is a low supply of CCN. Increasing concentrations can therefore impact droplet number concentrations and the downwelling longwave radiation of clouds significantly (Mauritsen et al, 2011). During the MOSAiC expedition in 2020, extreme values of aerosol particle concentrations for the Arctic were observed during a warm air intruision event (Dada et al., 2022), which also led to a significant increase in the CCN concentration. The definition of warm air intruisions is more broad than for AR as it does not limit the shape or moisture content of the air mass, and would in practice include most AR that reach the Arctic. In the Antarctic, there are several studies on AR impacts on ice shelf calving due to precipitation effects (e.g Wille et al., 2019, 2021, and 2022), but no discussion on the role of aerosol particle transport. This is likely because the Antarctic continent is surrounded by ocean and thus there are barely any large sources of pollution that could by transported poleward by AR. Nevertheless, in this study both poles are included for comparison and completeness.

The aim of this work is to investigate aerosol particle transport to the poles by AR. To what degree AR are polluted with particles when they reach the poles? Is the impact of the river on clouds, precipitation and surface temperature different between clean and polluted AR, as we would expect. Is this relation the same at both poles? To answer these questions, the output from NorESM2-LM historical experiment for the sixth Coupled Model Intercomparison Project (CMIP6) is used, in combination with an AR detection algorithm.

This study is a part of the project polARosol, which also includes a study by Lea Haberstock with the aim to investigate how AR properties and frequency will change in the future. The same model experiment is used in both studies for consistency, which is a limitation for this work in terms of the available data variables and model resolution, but allows for further conclusions to be drawn when combining the results presented here with Lea's work.

Methods

Data description and preprocessing

There is one key preprocessing step of this analysis, which is the AR detection. The detection script is written by Remy Lapere, following the AR definition and detection principle developed by Wille et al (2021). This principle is to detect AR by identifying regions of adjacent gridboxes that have high poleward integrated vapour transport (IVT) between certain pressure levels. IVT is given by

$$\text{IVT} = -\frac{1}{g}\int_{900\text{ hPa}}^{300\text{ hPa}} q\mathbf{V}dp$$

where g is the standard gravity, q is the specific humidity and **V** is the meridional wind component. Only the positive (poleward) wind is considered. In the original algorithm by Wille et al (2021), the IVT is calculated in each gridbox for a reference period, and the threshold for "high" IVT is set to the 98th percentile in each gridbox, calculated separately for each month. Then for the detection, clusters of gridboxes with an IVT above the threshold and that reach at least 20˚ latitude in size are considered to be AR, at each timestamp. Important to note is that this algorithm was developed for reanalysis data with 3 hourly output. In this project we wanted to be able to look at projections of future trends in AR (see Lea's report), and therefore we use model data, more specifically the NorESM2-LM output for the historical CMIP6 experiment (Lea also uses scenarioMIP for future trends). The highest temporal resolution avalaible is daily average output. So, the fluctuations in IVT in our data are dampened compared to what was used by Wille et al (2021), and what we can detect is only the daily averaged AR. Therefore, in the detection script used for this report the IVT threshold was set to the 94th percentile of each gridbox. This threshold was chosen by tuning the detection based on a comparison with a one-year AR detection product from Jonathan Wille, see the Supplementary material for details. However, in our detection scheme the threshold is not calculated separately for each month, but for the entire reference period which is 2000-2015. In the algorithm by Wille, the IVT and therefore also AR beyond latitude +/- 80 degrees are discarded, we have not made this cut. I¨n summary the AR detection used for this report has many drawbacks, not only because of the low temporal and spatial resolution of the data, and by the blunt threshold, but also because there simply is no defined objective detection method of AR, and results should be interpreted with this in mind.

In this report the period 1990-2015 is selected from the historical CMIP6 run. The AR detection script cannot be run in the conda environment set up for this course so I have run it locally, and therefore the pre-processed files `historical_1990-2000_combined_q94.nc` and `historical_2000-2015_combined_q94.nc` are provided (they are split in 2 simply to not run into issues with file size, I combine them below). These make an AR mask, where the parameter `ivt` is 1 for every gridbox part of an atmospheric river at a given timestamp, and 0 otherwise. They were obtained with the script `opencv_detection_OK.py` (by Remy Lapere), also provided.

The choice variables used for classification of polluted vs clean AR, as well as for the analysis on the impact, is limited by what variables that are available with daily time resolution. Therefore, the aerosol optical depth (AOD) at 550 nm will be used to sort the AR, further described in the section AR masking and pollution threshold. To investigate the impact of aerosol particle transport in AR, the variables cloud fraction, precipitation rate, surface temperature and downwelling longwave radiation flux will be used.

Loading data

[1]:
```
import xarray as xr
import pandas as pd
import numpy as np
import matplotlib.pyplot as plt
import matplotlib.path as mpath
import s3fs
import intake
import functions_JA as fun
import warnings
import cartopy.crs as ccrs
import os
```

[2]:
```
#Years considered, corresponding to AR mask
start_year=1990
end_year=2015
```

Loading AR mask, pre calculated as described:

[3]:
```
#loading both mask files into one dataset
ar_mask = xr.open_mfdataset('historical_*_combined_q94.nc')
```

Fetching AOD data from met.no:

[4]:
```
#Define connection to met.no bucket
#Key and sectret are in file passwords.txt so they are hidden
passwords = np.loadtxt('passwords.txt', dtype='str')
s3 = s3fs.S3FileSystem(key=passwords[0],
                       secret=passwords[1],
                       client_kwargs=dict(endpoint_url="https://rgw.met.no"))

#path to aod data file, in Ada's folder
s3path_aod = 's3://escience2022/Ada/monthly/'+ \
'od550aer_AERday_NorESM2-LM_historical_r1i1p1f1_gn_19500101-20141231.nc'

#Importing file and dropping unused parameters
aod_ds = xr.open_dataset(s3.open(s3path_aod),
                         drop_variables =['time_bnds','lat_bnds','lon_bnds'])
#Selecting the right time period
aod_ds = aod_ds.sel(time =
                    slice(str(start_year)+"-01-01", str(end_year-1)+"-12-31") )
```

In this AOD file, the timestamp is at midnight every day while the AR mask has timestamps at noon, even though it is the same model run with daily average output. Therefore I replace the AOD time with the time-array from the AR mask, as this will simplify the masking:

[5]:
```
aod_ds['time'] = ar_mask.time
```

Loading variables to be considered, from pangeo:

[ ]:
```
#Define url and connection
cat_url = "https://storage.googleapis.com/cmip6/pangeo-cmip6.json"
col = intake.open_esm_datastore(cat_url)

#Search database for the right model, experiment and variables.
#Save catalog as dictionary, and finally as xarray dataset
cat = col.search(source_id=['NorESM2-LM'],
                 experiment_id=['historical'],
                 table_id=['day'],
                 variable_id=['clt','pr','tas','rlds'],
                 member_id=['r1i1p1f1'])
dset_dict = cat.to_dataset_dict(zarr_kwargs={'use_cftime':True})
dataset_list = list(dset_dict.keys())
dset = dset_dict[dataset_list[0]]
vars_ds = dset.sel(member_id='r1i1p1f1',
                   time=slice(str(start_year)+"-01-01",␣
 ↪str(end_year-1)+"-12-31"))
```

```
--> The keys in the returned dictionary of datasets are constructed as follows:
        'activity_id.institution_id.source_id.experiment_id.table_id.grid_label'
```

```
<IPython.core.display.HTML object>
```

```
<IPython.core.display.HTML object>
```

AR masking and pollution threshold

Since I want to investigate the properties of clean versus polluted AR, I now need to sort the detected AR depending pollution level. As previously mentioned, aerosol particle concentrations at the poles are generally very low, so low that air transported from mid latitudes will almost always be polluted in comparison. This means that setting the pollution thresholds based on high and low polar concentrations would classify >95% of AR as polluted (yes, I tried), making it difficult to study differences between pollution levels. Therefore, I define the thresholds for clean and polluted AR based on the AOD at mid latitudes. AR that reach the Arctic (above 60° North) are considered polluted if the average AOD in the river is above the 95th percentile of AOD for the whole time period at latitudes between 30° and 60° North. Arctic AR with an average AOD below the 25th percentile are considered clean. Antarctic AR are sorted depending on the AOD between 30° and 60° South, with a pollution threshold of the average AOD and clean rivers below the 10th percentile. The lower thresholds for the Antarctic were tuned in order to obtain a significant fraction of polluted AR.

[7]:
```
#Creating a dictionary to store the pollution limits for the sorting of ARs
#skipna default for float dtypes
aod_lim= {}
aod_lim['midlat_75th'] = aod_ds.sel(lat =
                                    slice(30,60)).od550aer.quantile(0.75)
aod_lim['midlat_25th'] = aod_ds.sel(lat =
                                    slice(30,60)).od550aer.quantile(0.25)
```

```
aod_lim['midlowlat_75th'] = aod_ds.sel(lat =
                                       slice(-60,-30)).od550aer.quantile(0.75)
aod_lim['midlowlat_25th'] = aod_ds.sel(lat =
                                       slice(-60,-30)).od550aer.quantile(0.25)
```

[8]:
```
aod_lim['midlat_mean'] = aod_ds.sel(lat = slice(30,60)).od550aer.mean()
aod_lim['midlowlat_mean'] = aod_ds.sel(lat = slice(-60,-30)).od550aer.mean()
aod_lim['midlowlat_10th'] = aod_ds.sel(lat =
                                       slice(-60,-30)).od550aer.quantile(0.1)
```

Now I can apply the AR mask to the AOD data and sort the rivers. The function `sort_ar_by_aod` takes the AOD dataset, the AR mask and the pollution limits, loops over every timestep, applies the mask and then checks the average AOD of every river to sort it. Returned is an AOD dataset with all gridboxes outside the rivers masked out, separated into polluted, clean, and intermediate pollution levels. These parameters can be used as an AR mask for each pollution category separately. There is also a count of the number of rivers in each category for every timestep.

[9]:
```
arc_aod_ar = fun.sort_ar_by_aod(aod_ds.sel(lat=slice(60,90)),
                                ar_mask.sel(lat=slice(60,90)),
                                aod_lim['midlat_mean'],
                                aod_lim['midlat_25th'])
ant_aod_ar = fun.sort_ar_by_aod(aod_ds.sel(lat=slice(-90,-60)),
                                ar_mask.sel(lat=slice(-90,-60)),
                                aod_lim['midlowlat_mean'],
                                aod_lim['midlowlat_10th'])
```

Next I have to apply the AR masks to the dataset containing the variables of interest. The masked datasets are stored in two different dictionaries, one for each pole. In order to plot histograms of the variables they need to be in 1-dimensional arrays, with all NAN-values (from the masked out data) removed. These are also stored in the dictionaries, to simplify plotting.

[10]:
```
#Create empty dictionaries to fill with variables and define variables
#and pollution levels considered:
arc_plotting_vars = {}
ant_plotting_vars = {}
flat_vars = ['clt','pr','tas','rlds']
levs = ['clean','mid','poll']


for lev in levs:
    #Create a dictionary in each pollution level
    arc_lev_dict = {}
    ant_lev_dict = {}

    #Mask the dataset with the AR mask for current pollution level,
    #separate for both poles and store in dictionary created above.
    arc_lev_dict['ar_masked'] = \
    vars_ds.sel(lat=slice(60,90)).where(arc_aod_ar[f'{lev}_ar_aod'].notnull() )
```

```
    ant_lev_dict['ar_masked'] = \
    vars_ds.sel(lat=slice(-90,-60)).where(ant_aod_ar[f'{lev}_ar_aod'].notnull() )

    for var in flat_vars:
        #For current variable, flatten the masked array and remove NaN values
        arc_i = ~np.isnan(arc_lev_dict['ar_masked'][var].values.flatten())
        arc_lev_dict[f'{var}_flat']= \
        arc_lev_dict['ar_masked'][var].values.flatten()[arc_i]
        ant_i = ~np.isnan(ant_lev_dict['ar_masked'][var].values.flatten())
        ant_lev_dict[f'{var}_flat']= \
        ant_lev_dict['ar_masked'][var].values.flatten()[ant_i]

        if var == 'pr':
            #Convert precipiation from kg/m^2/s to mm/day
            arc_lev_dict[f'{var}_flat']= arc_lev_dict[f'{var}_flat']*86400
            ant_lev_dict[f'{var}_flat']= ant_lev_dict[f'{var}_flat']*86400

    #save dictionary of data in current pollution level
    arc_plotting_vars[lev]=arc_lev_dict
    ant_plotting_vars[lev]=ant_lev_dict
```

Results and discussion

[11]:
```
#Selecting one timestamp and just each respective pole from the AR mask dataset:
arc_ex_ar = ar_mask.sel(time = '2014-06-12', lat =slice(65,90))
ant_ex_ar = ar_mask.sel(time = '2014-06-30', lat =slice(-90,-65))

#putting in dictionaries to simplify simultaneous plotting
plot_ex_ar= {'Arctic' :arc_ex_ar, 'Antarctic' : ant_ex_ar}

#MAking figure, adding the two subplots and setting their extent separately
#as they have different projections:
fig = plt.figure(figsize = (10,5), dpi=100)

arc_ax = fig.add_subplot(121, projection=ccrs.NorthPolarStereo())
ant_ax = fig.add_subplot(122, projection=ccrs.SouthPolarStereo())

arc_ax.set_extent([0, 360, 65, 90], ccrs.PlateCarree())
ant_ax.set_extent([0, 360, -65, -90], ccrs.PlateCarree() )

axs=[arc_ax,ant_ax]
#looping over the keys in the dictionary and
#plotting each dataset in the respective axis:
for i, pole in enumerate(plot_ex_ar.keys()):
    axs[i].coastlines(linewidth=0.5)
    #Just a function so that the extent is cut out as a circle instead of square:
```

```
    fun.circle_for_polar_map(axs[i])
    axs[i].set_title(pole)
    axs[i].pcolormesh(plot_ex_ar[pole].lon,
                      plot_ex_ar[pole].lat,
                      plot_ex_ar[pole].ivt.squeeze(),
                      cmap='Blues', vmin=0,vmax=1,
                      transform=ccrs.PlateCarree() )
    #adding the text showing the timestamp:
    fig.text(0.1,-0.05,plot_ex_ar[pole].time.values.astype('datetime64[D]')[0],
             horizontalalignment='left',verticalalignment='bottom',
             transform=axs[i].transAxes)
plt.show()
```

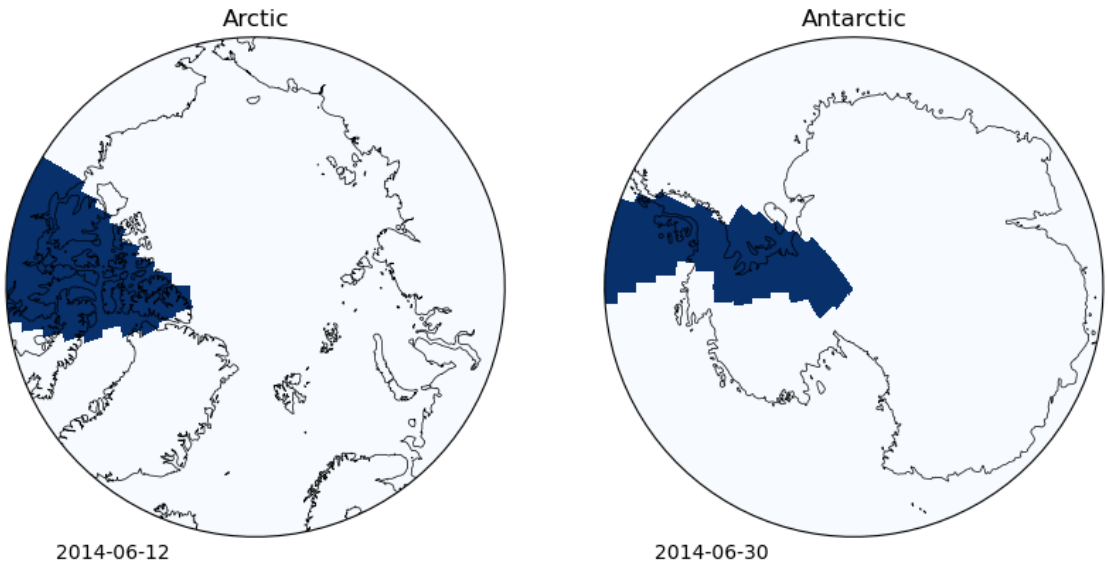

Figure 1: An example of detected AR. For each pole one snapshot at different is plotted, showing all gridboxes detected as part of an AR in blue.

To visually demonstrate the AR detection, the AR mask is plotted for one timestamp for each pole featuring a detected AR in blue in figure 1. This figure demonstrates two main issues with the current detection scheme, that some rivers are too wide (left), and that many reach the center of the pole (right). The latter is an issue because since only the meridional wind component is considered, detected AR can by definition not cross the pole. In reality, it is also very rare that they actually reach this far, a few times per year at most. Wille et al (2020) deal with this problem by not considering latitudes beyond 80° North or South. We did not make this cut as we wanted to include events such as the one observed during MOSAiC (Dada et al, 2022), where the warm moist air mass almost reached the North pole. However, this results in the artifact that the AR converge and end at the pole. On the other hand, a cut at 80° creates the artefact that AR end there. In this study, this illusion of a polar AR singularity is most likely not the biggest uncertainty and we have not made any attempts at finding a way to avoid it. But in a larger context, it highlights a flaw in the original algorithm by Wille et al, and raises philosophical questions about the very definition

of AR. If they are defined by poleward moisture transport, then they can actually theoretically never cross the poles. But in practice, long moist air corridors probably don't care about this definition and sweep over the poles if they desire. Again this would be a quite rare event and not the most important aspect of AR to consider, but it is something to keep in mind when defining future detection schemes or attempting to model AR. One solution, used by Mattingly et al. (2018), is to allow negative meridional winds above a certain latitude, to feature curvature of AR.

The issue of the detected rivers being too wide is more alarming. It is also related to the issue of the pole, as it is an indication that the detection scheme is not strict enough and classifies too large regions as AR. There is no strict threshold of the accepted width of AR, but they are defined as narrow and I think the river in the left plot does not objectively fit that description. One potential method to reduce the size of detected AR would be to increase the IVT threshold, currently at the 94th percentile. The reason for keeping it this low is because even at this threshold, the number of detected rivers is seemingly too low (see the Supplementary material), which probably has to do with the low time resolution of the input data. Instead, I think the AR size could be improved by separating the IVT values monthly, like in the algorithm by Wille et al (2021) (this was not done from the beginning because it was initially overlooked and once discovered, not trivial to implement). IVT is likely to vary between seasons as the specific humidity depends on temperature. So, the IVT threshold may be unproportionally high during winter when the air is dryer, leading to very few AR detections, with the opposite effect during summer. To look at how the number of detected AR varies seasonally, the total number of detected rivers in each month during the whole time period, separated by pollution category, is plotted in figure 2.

[12]:
```
labels=['Jan','Feb','Mar','Apr','May','June','July','Aug','Sep','Oct','Nov','Dec']

#Grouping the polar AR AOD datasets by month and summing over the whole period
arc_monthly_count = arc_aod_ar.groupby('time.month').sum(dim='time')
ant_monthly_count = ant_aod_ar.groupby('time.month').sum(dim='time')

#defining a function that plots all three pollution levels in the given
#grouped dataset on a given axis, just to avoid writing the code twice
def plot_count_bar(ax ,labels, grouped_ds, title=''):
    ax.bar(labels, grouped_ds.clean_ar_counts.values, label='Clean')
    ax.bar(labels, grouped_ds.mid_ar_counts.values,
           bottom = grouped_ds.clean_ar_counts.values,
           color='tab:green', label='Intermediate')
    ax.bar(labels, grouped_ds.poll_ar_counts.values,
           bottom = grouped_ds.clean_ar_counts.values+\
           grouped_ds.mid_ar_counts.values,
        color='tab:orange', label='Polluted')
    ax.set_xticklabels(labels, rotation=45)
    ax.set_title(title)

#PLotting for both poles
fig, axs = plt.subplots(1,2, figsize=(11,4),dpi=100, sharey=True)
plot_count_bar(axs[0], labels, arc_monthly_count, 'Arctic')
plot_count_bar(axs[1], labels, ant_monthly_count, 'Antarctic')
axs[0].set_ylabel('Number of AR')
```

```
fig.suptitle('Number of atmospheric rivers detected, by month')
plt.legend()
plt.show()
```

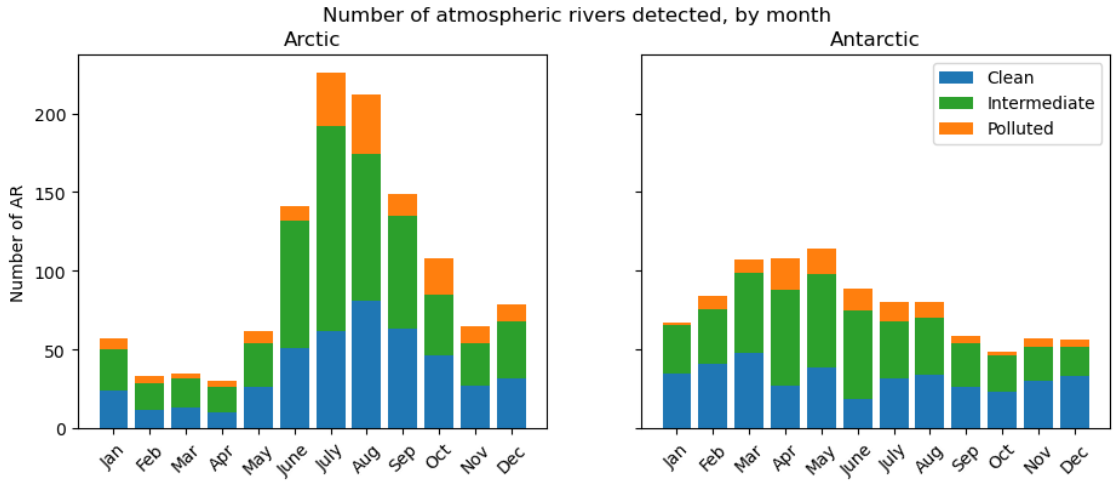

Figure 2: Total number of detected AR in each pollution category summed for every month between 1990-2015, above 60˚ North (left) and below 60˚ South (right). Polluted AR in the Arctic are defined by an average AOD above the 75th percentile of AOD values between 30˚ and 60 ˚ North, clean rivers below the 25th percentile, and remaining AR are classed as intermediate. In the Antarctic, AR are considered polluted with an average AOD above the mean AOD between 30˚ and 60 ˚ South. Clean AR are defined as below the 10th percentile of AOD in the same region, and all AR in between are considered intermediate.

This plot shows a big difference in AR trends between the poles. The left panel clearly shows that in the Arctic, AR are much more common in the summer than in the winter. This is in line with what I discussed above, and could therefore be due to the fact that the IVT threshold applied is not adjusted monthly. However, the same trend is not seen at all in the right panel, for the Antarctic. In fact, AR seem to be the least frequent during the southern hemispheric summer, with the peak in the fall. Overall the seasonal trend is also much less pronounced, and the number of AR more constant throughout the year. This could be an indication that the annual cycle detected in the Arctic is real and not an artifact due to the IVT threshold. But it could also just mean that the IVT has a less pronounced annual cycle in the Antarctic, and the AR detection is therefore less sensitive to the seasonality of the IVT threshold. The Antarctic is surrounded by ocean rather than land, and the surface temperature does not vary as much over ocean. Or, the trend in IVT has less to do with temperature and more to do with large scale atmospheric modes like the Antarctic and Arctic Oscillation, in which case it is also hard to say whether the trends observed here are real or caused by the static IVT threshold.

In any case, this is the distribution of AR in the data for this study, which should be kept in mind when considering the results of the next analysis, which is a comparison of the cloud and precipitation variables in the gridboxes of polluted versus clean AR, for two different seasons.

[36]:
```
flat_vars = ['clt','pr','tas','rlds']
seasons = [[11,12,1,2],[5,6,7,8]]
#Using a function to plot the histogram, that loops over variables in the given
#dictionary and uses the AOD AR dataset to sum the AR counts in each category
#and plot the pie chart:
fun.plot_hist(flat_vars,seasons,
              arc_plotting_vars,
              arc_aod_ar,
              'arctic_vars', 'Arctic')
```

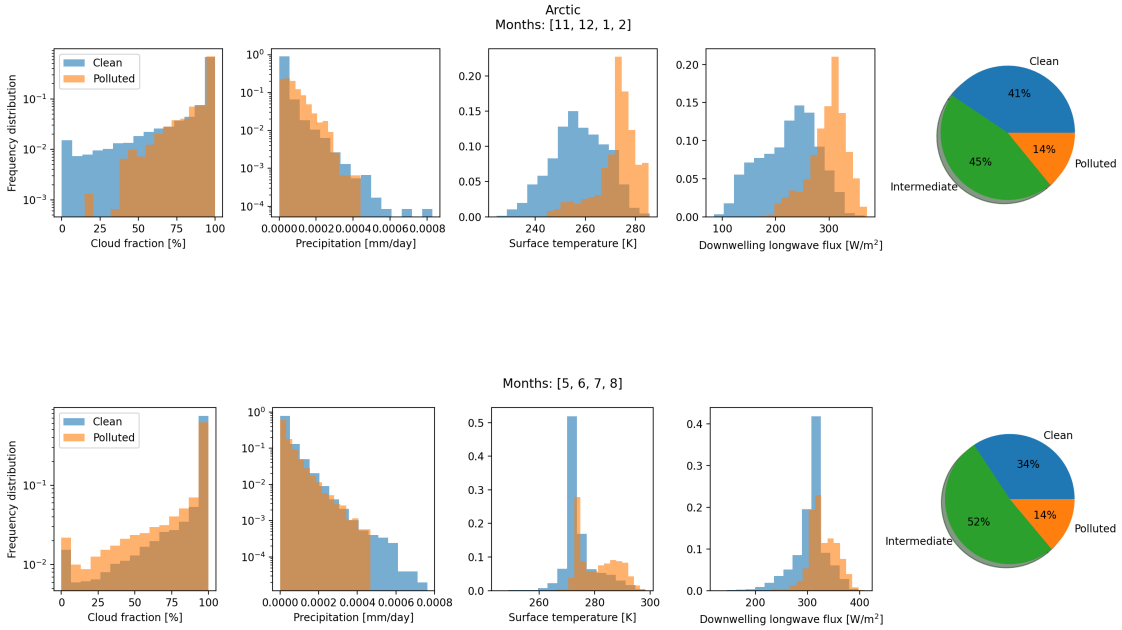

Figure 3: Comparison of the distribution of values of cloud fraction, precipitation, surface temperature, and downwelling longwave radiation between clean and polluted detected AR, plotted for the winter (top) and summer (bottom) season in the Arctic (above 60˚ North). Pie charts to the right show the fractions of the pollution categories of detected AR during the respective season. Polluted AR in the Arctic are defined by an average AOD above the 75th percentile of AOD values between 30˚ and 60 ˚ North, clean rivers below the 25th percentile, and remaining AR are classed as intermediate.

The plot above is for the Arctic, the upper row corresponds to the winter season, and the bottom summer. In each of the four left panels in every row, the distribution of values for the corresponding parameter found within polluted and clean AR, respectively, are plotted. Given the high moisture content of AR, I expected a shift towards higher cloud cover with increased number of particles. What we can see is actually just a very small such shift in winter, while during summer, high cloud cover is actually more common in clean AR. Important to note is that the cloud fraction variable takes the entire column into account, while we only detect AR between 300 and 900 hPa. It would therefore be better to look at a vertically resolved parameter that indicates cloud presence such as droplet number concentration in order to determine if the shifts we see in cloud cover can really be appointed to the pollution brought in by AR. Especially since the pollution levels are

also defined by aerosol load in the whole column, in the form of AOD. This also means that higher AOD does not necessarily mean higher number concentration of particles in general and CCN in particular inside the AR. Furthermore, a shift from fewer and larger to many and smaller cloud droplets does not necessarily have to effect the cloud fraction, even though we thought it would. Given these substantial uncertainties and that the difference we see is so small, I would say that this result is inconclusive.

The result of the comparison of precipitation rate is almost as vague, but during the winter season it is clear that very low precipitation rates are less common in polluted than clean AR. Very high precipitation rates are on the other hand also more common in clean rivers. During the summer we see the same relationship, much less pronounced to the point where it is barely noticable in the log scale. The expected relationship between precipitation rate and pollution is dependent on the relationship for cloud parameters. With more CCN, there are more and smaller droplets, which delays precipitation. But as we don't see a strong shift in cloud cover, there is actually not much to expect in the precipitation rate, which is in line with what we see.

The most significant shift in the distribution is found for surface temperature and downwelling longwave flux, during winter season. I had not intitially expected the surface temperature differ very much between polluted and clean AR, but with an increase in downwelling longwave it makes sense. The question is now whether the increase in longwave flux is a direct aerosol effect or secondary due to altered cloud properties. Since the results of the cloud cover comparison are inconclusive it is impossible to rule out one or the other, but it can at least be said that it is reasonable to see the strongest shift in winter, as the surface temperature is then more strongly dependent on longwave radiation, due to the absence of incoming shortwave radiation. During summer the strongest peaks in temperature and longwave flux coincide for both pollution categories, so there is most likely other factors dominating these variables. But there is a second peak that is shifted similar to in the winter season, which could have the same cause. Another possible explanation for the shift in temperature is that the more polluted AR are at lower latitude, and therefore have a lower temperature. This should be tested in future studies for example by comparing high and low AOD regions with the same latitude cut without AR detection.

[ ]:
```
fun.plot_hist(flat_vars,seasons,
              ant_plotting_vars,
              ant_aod_ar,
              'antarctic_vars', 'Antarctic')
```

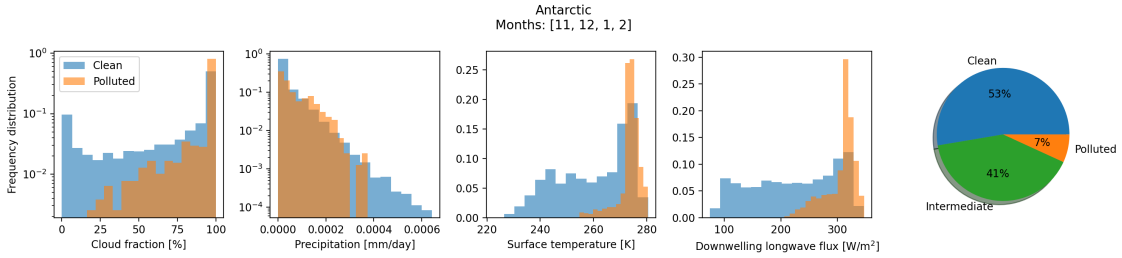

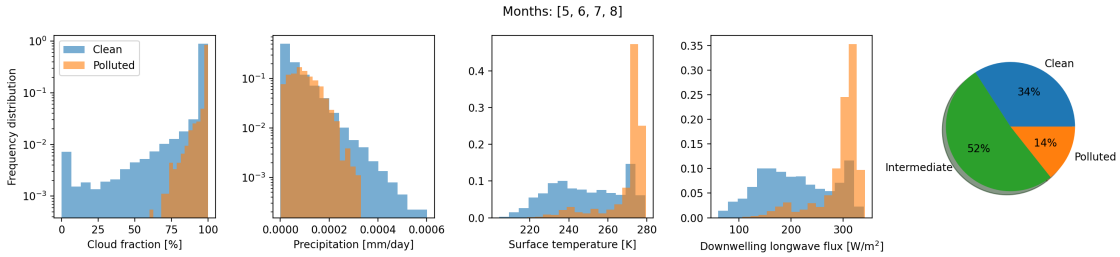

Figure 4: Comparison of the distribution of values of cloud fraction, precipitation, surface temperature, and downwelling longwave radiation between clean and polluted detected AR, plotted for the summer (top) and winter (bottom) season in the Antarctic (below 60˚ South). Pie charts to the right show the fractions of the pollution categories of detected AR during the respective season. AR in the Antarctic are considered polluted with an average AOD above the mean AOD between 30˚ and 60 ˚ South. Clean AR are defined as below the 10th percentile of AOD in the same region, and all AR in between are considered intermediate.

This figure is the same as described above, but for the Antarctic. Note the similar fractions of clean, intermediate and polluted AR as in the Arctic, even though the pollution threshold is a lot lower and the requirements for clean AR are much more strict. The comparisons of cloud cover and precipitation rate are quite similar as for the Arctic, and do not result in any strong conclusions, although it is notable that the shift in cloud cover is here consistently to the right for polluted AR. Most significant are again the differences in surface temperature and downwelling longwave flux, even though the distributions look very different than in the Arctic. Just like the seasonal trend in AR frequency, the shift in surface temperature and downelling longwave flux is more constant throughout the seasons, and the peak coincides between clean and polluted AR. However, the distribution between the pollution levels is clearly different.

The fact that it differs so much between the Arctic and Arctic is an indication that the effect of aerosols is significant, since the Antarctic is so much cleaner. Howver, more tests are needed to rule out other explanations, if the temperature gradient between latitudes in the Antarctic region is lower than it could still be due to to a difference in latitude between clean and polluted AR. Furthermore, the shifts in distribution we see could just be becuase of the difference in AOD, and not necessarily correlated with the high moisture transport. This can be tested by doing the same tests outside of detected AR.

If it can be confirmed that the shift in the distributions of longwave radiation and surface temperature are in fact at least partly due to aerosol transport by AR, then it should be tested for statistical significance.

Summary and conclusions

An AR detection scheme has been applied to the 25 years (1990-2015) of daily output data from NorESM2, the Historical CMIP6 experiment. The polar regions were selected and detected AR were sorted into clean, polluted and intermediate, using AOD. The distribution of cloud fraction, precipitation rate, surface temperature and downwelling longwave radiation values was compared between clean and polluted AR, and the number of AR detected in each pollution category in every month was counted to study the seasonal pattern. The AR detection scheme was also discussed.

Results from this study indicate that the seasonal occurance of AR differs a lot between poles, with more than twice as many AR in summer months than winter months in the Arctic, and a much more even yearly distribution of AR frequency in the Antarctic. Impacts of aerosol transport by AR seem most relevent to study in the Arctic, as AOD within Ar is much higher than in the Antarctic. AR with high average AOD are associated with increased surface temperature and downwelling longwave radiation. This could be due to a positive cloud feedback, although no significant differnce was found in precipitation and cloud fraction. The comparisons made should also be done using the data without the AR mask and outside of the AR, to see if the observed shifts are indeed due to a feedback induced by a combination of AR and high AOD, or just a pure AOD effect, or just a latitudinal effect due to higher AOD at lower latitudes with lower temperature.

This work is highly limited by the variables available, the low temporal resolution, and perhaps most importantly the AR detection scheme used. My results are an indication of where focus could lay in future studies, for which the detection scheme must be further developed. Currently, detected AR are too wide and too long, yet too few. Possible improvements should therefore include a monthly resolved threshold for high IVT, a way to limit the width to length ratio if still necessary, as well as a strategy to deal with AR approaching the poles. The latter is complex as it involves the very definition of AR as poleward moisture transport, but could perhaps be dealt with by calculating IVT also with negative meridional winds, just around the poles. I think this is something to discuss in a larger context, as studies use vastly different detection schemes that rely on different definitions of AR, making them difficult to compare.

To improve this study and properly investigate the role of aerosol transport by AR I think it would be necessary to use data with higher temporal and spatial resulotion, like reanalysis or a nudged model run with hourly output. Not only would it mot likely improve the detection, which could then also be checked by comparing to observations, but it would also allow for using more diagnostic variables. For example, cloud droplet and CCN concentration, and a vertically resolved aerosol concentration. I think this is necessary to actually correlate the high concentration of aerosols with AR, and even study how aerosols are picked up and transported with AR.

Acknowledgements

A huge thank you to Remy Lapere for bringing the inspiration for the entire project, writing the AR detection script, and for wonderful and much needed guidance and support throughout the work with this study. A major thanks also to Lea Haberstock, it was a pleasure working together and thank you for all of the fruitful discussions and for your patience with me. This project would not have been possible without Jonathan de Wille, not only was his work a key inspiration but he also deserves a lot of credit for sharing a detection product with us, thank you! Finally, thank you to everyone involved in the eScience course, to Paul Zieger and Michael Schultz for organizing, to all lecturers and assistants for help and inspiration (especially Ada for getting us the right AOD data, thanks!!), and to all the students for making it a really fun course with so many great projects, discussions, and good times! A special little thank you to all the Love is blind fans for the best company, also, you are welcome.

References

Nash, D., Waliser, D., Guan, B., Ye, H., & Ralph, F. M. (2018). The role of atmospheric rivers in extratropical and polar hydroclimate. Journal of Geophysical Research: Atmospheres, 123, 6804–

6821. https://doi.org/10.1029/2017JD028130

Payne, A.E., Demory, ME., Leung, L.R. et al. Responses and impacts of atmospheric rivers to climate change. Nat Rev Earth Environ 1, 143–157 (2020). https://doi.org/10.1038/s43017-020-0030-5

Wille, J.D., Favier, V., Dufour, A. et al. West Antarctic surface melt triggered by atmospheric rivers. Nat. Geosci. 12, 911–916 (2019). https://doi.org/10.1038/s41561-019-0460-1

Neff, W. Atmospheric rivers melt Greenland. Nature Clim Change 8, 857–858 (2018). https://doi.org/10.1038/s41558-018-0297-4

Mauritsen, T., Sedlar, J., Tjernström, M., Leck, C., Martin, M., Shupe, M., Sjogren, S., Sierau, B., Persson, P. O. G., Brooks, I. M., and Swietlicki, E.: An Arctic CCN-limited cloud-aerosol regime, Atmos. Chem. Phys., 11, 165–173, https://doi.org/10.5194/acp-11-165-2011, 2011.

Dada, L., Angot, H., Beck, I. et al. A central arctic extreme aerosol event triggered by a warm air-mass intrusion. Nat Commun 13, 5290 (2022). https://doi.org/10.1038/s41467-022-32872-2

Wille, J. D., Favier, V., Gorodetskaya, I. V., Agosta, C., Kittel, C., Beeman, J. C., et al. (2021). Antarctic atmospheric river climatology and precipitation impacts. Journal of Geophysical Research: Atmospheres, 126, e2020JD033788. https://doi.org/10.1029/2020JD033788

Wille, J.D., Favier, V., Jourdain, N.C. et al. Intense atmospheric rivers can weaken ice shelf stability at the Antarctic Peninsula. Commun Earth Environ 3, 90 (2022). https://doi.org/10.1038/s43247-022-00422-9

Mattingly, K. S., Mote, T. L., & Fettweis, X.(2018). Atmospheric river impacts onGreenland Ice Sheet surface massbalance.Journal of GeophysicalResearch: Atmospheres,123, 8538–8560.https://doi.org/10.1029/2018JD028714

Supplementary material

Here I will demonstrate some of the testing I did before settling on using the 94th percentile (hereafter q94) as the threshold for IVT in the AR detection scheme. Jonathan de Wille provided us with a one year AR mask calculated on ER5 reanalysis data, using the detection scheme from de Wille et al., 2021. The year is 2020, and this data set will be referred to as the 2020 detection product. I used this dataset to estimate the expected number of AR events per year, and to compare spatial extension and distribution of AR. For simplicity I will only show this process for the Arctic.

When we fist tested the detection scheme used in this report, we knew that the 98th percentile used by Wille et al was most likely to high since it was used on 3-hourly data. Still we tried it, and got barely any AR. Therefore we moved on to lower thresholds around q90-q95 to test the sensitivity. Below I test with q92, q93 and q94 for one year, 2014, and the ar masks have been previously calculated used the detection script described in the Methods section, but with the respective thresholds.

[23]:
```
#Load 2020 detection product
AR_2020_file = 'AR_detection_2020.nc4'
data_dir = '/home/jovyan/Tjaernoe2022-group5/data'
ar_2020 = xr.open_dataset(os.path.join(data_dir,AR_2020_file))
```

[24]:
```
#Count atmospheric rivers above 60 latitude, using function
counted_2020 = fun.count_2020_ARs(ar_2020,60)
```

[25]:
```
#Load previously calculated ar masks with different IVT thresholds.
hist_q92 = xr.open_dataset('historical_2014_q92.nc')
hist_q93 = xr.open_dataset('historical_2014_q93.nc')
hist_q94 = ar_mask.sel(time= slice('2014-01-01','2014-12-31'))
```

[26]:
```
#Count all the AR. Function returns the dataset input,
#with counts as added variable.
counted_q92 = fun.count_ARs(hist_q92, 60)
counted_q93 = fun.count_ARs(hist_q93, 60)
counted_q94 = fun.count_ARs(hist_q94, 60)
```

One way to determine if the chosen threshold is appropriate is to check the number of detected AR and compare to the 2020 detection product. Of course they are from different years (2014 vs 2020), but I assume they should be comparable. Since the 2020 AR mask is three hourly, simply adding the counts and compare to the 2014 daily data would not be fair. The detection file is just a binary mask for ever gridcell, AR or not, so it is not really possible to compute daily average ARs and then compare. Therefore, I just divide the 2020 counts by $\frac{24}{3} = 8$.

[27]:
```
print('counts in 2020 product: ',counted_2020.ar_counts_60.sum().values/8)
print('counts in 2014 historical with q94: ',
      counted_q94.ar_counts_60.sum().values)
print('counts in 2014 historical with q93: ',
      counted_q93.ar_counts_60.sum().values)
print('counts in 2014 historical with q92: ',
      counted_q92.ar_counts_60.sum().values)
```

```
counts in 2020 product:  166.5
counts in 2014 historical with q94:  81.0
counts in 2014 historical with q93:  105.0
counts in 2014 historical with q92:  140.0
```

As seen above, the number of detected reivers in the 2020 product is similar to the number in 2014 with the q92 threshold applied, while only about half as many rivers are detected with the q94 threshold. Since we are using hourly averaged data we should probably detect a slightly lower number of AR, but still, based on only the the count I still would have chosen a lower threshold like q93 or even q92 to capture as many as possible and have more data. However, I also needed to make sure that we don't have an over detection. To check this I looked at the entire year (2014) of detected rivers with the different thresholds using animations. Figure S1 shows a snapshot of one timestamp with the different thresholds applied to demonstrate this process. Plotted is also one timestamp with 2 AR in the 2020 detection product, for qualitative comparison.

[28]:
```
#I think plot snapshot of 1 day instead
f,ax = plt.subplots(1,4,dpi=100, figsize =(15,5),
            subplot_kw={'projection':ccrs.Orthographic(central_latitude=90.0)})
counted_q94.sel(lat=slice(40,90),
                time = '2014-07-04').ivt.squeeze().plot.pcolormesh(
```

```
    cmap = plt.get_cmap('Blues'),ax=ax[0],
    transform=ccrs.PlateCarree(),
    add_colorbar= False,
    vmin=0,vmax=1
)

counted_q93.sel(lat=slice(40,90),
                time = '2014-07-04').ivt.squeeze().plot.pcolormesh(
    cmap = plt.get_cmap('Blues'),ax=ax[1],
    transform=ccrs.PlateCarree(),
    add_colorbar= False,
    vmin=0,vmax=1
)

counted_q92.sel(lat=slice(40,90),
                time = '2014-07-04').ivt.squeeze().plot.pcolormesh(
    cmap = plt.get_cmap('Blues'),ax=ax[2],
    transform=ccrs.PlateCarree(),
    add_colorbar= False,
    vmin=0,vmax=1
)
time_2020 = '2020-04-15T15:00:00.000000000'
counted_2020.sel(lat=slice(40,90),
                 time = time_2020).ar_binary_tag.squeeze().plot.pcolormesh(
    cmap = plt.get_cmap('Blues'),ax=ax[3],
    transform=ccrs.PlateCarree(),
    x='lon',y='lat',
    add_colorbar= False,
#    vmin=0,vmax=1
)
for a in ax:
    a.coastlines()
    fun.circle_for_polar_map(a)
    a.set_extent([0, 360, 40, 90], ccrs.PlateCarree())
    gl = a.gridlines(draw_labels=True)
    #a.add_feature(cy.feature.BORDERS)

ax[0].set_title('Historical q94 \n 2014-07-04')
ax[1].set_title('Historical q93 \n 2014-07-04')
ax[2].set_title('Historical q92 \n 2014-07-04')
ax[3].set_title('2020 product \n 2020-04-15')

gl.top_labels = False
gl.right_labels = False

plt.tight_layout()
plt.show()
```

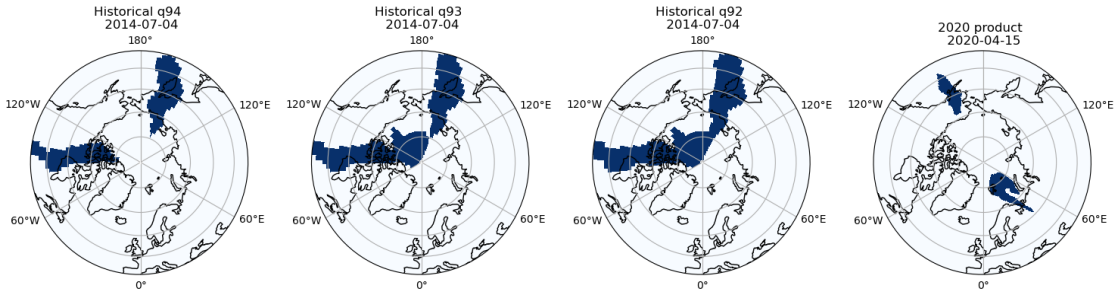

Figure S1: Snapshot of detected AR. Left three maps made using the detection scheme used in this study, with different thresholds for minimum IVT applied, the 94th, 93rd and 92nd percentile, respectively. The last figure is a snapshot from the 2020 detection product provided by Jonathan de Wille, using Wille et al., 2021, detection scheme on 3-hourly reanalysis data.

As previously mentioned, one issue with our detection scheme is that so many AR reach the pole, which is not only unrealistic but also conceptually not so great because by definition, the detected AR can never cross the pole. In the timestamp plotted in figure S1, this issue arises when applying th eq93 and q92 threshold, but not with q94. The shape and extent of the AR also seem more realistic with q94, in the two other versions the 2 detected rivers at this timestamp merge together and have a more broad and less defines shape. Especially compared to the 2020 product, where acompletely different timestamp is plotted, but it is still an indication of the refined shape of the detected AR using Wille et al., 2021 detection algorithm. There are many other timestamps when the Ar detected using the q94 threshold do reach the poles, and when they appear much too broad to be realistic (As shown in Figure 1). However, figure S1 is a representative example of the process that led to the choice of q94. Because of the low number of detected AR, I wanted to use a lower threshold, but as we can see, the risk for over detection is much bigger.

[29]:
```
f,ax = plt.subplots(1,4,dpi=100, figsize =(15,5),
                    subplot_kw={'projection':ccrs.Orthographic(central_latitude=90.
 ↪0)})
counted_q94.sel(lat=slice(40,90)).ivt.mean(dim='time').plot.pcolormesh(
    cmap = plt.get_cmap('Blues'),ax=ax[0],
    cbar_kwargs={
        'label':'AR occurence Frequency',
        'orientation':'horizontal',
    },
    transform=ccrs.PlateCarree(),
    x='lon',y='lat',
    levels = 8
)
counted_q93.sel(lat=slice(40,90)).ivt.mean(dim='time').plot.pcolormesh(
    cmap = plt.get_cmap('Blues'),ax=ax[1],
    cbar_kwargs={
        'label':'AR occurence Frequency',
        'orientation':'horizontal',
```

```
    },
    transform=ccrs.PlateCarree(),
    x='lon',y='lat',
    levels = 8
)
counted_q92.sel(lat=slice(40,90)).ivt.mean(dim='time').plot.pcolormesh(
    cmap = plt.get_cmap('Blues'),ax=ax[2],
    cbar_kwargs={
        'label':'AR occurence Frequency',
        'orientation':'horizontal',
    },
    transform=ccrs.PlateCarree(),
    x='lon',y='lat',
    levels = 8
)
counted_2020.ar_binary_tag.mean(dim='time').plot.pcolormesh(
    cmap = plt.get_cmap('Blues'),ax=ax[3],
    cbar_kwargs={
        'label':'AR occurence Frequency',
        'orientation':'horizontal',
    },
    transform=ccrs.PlateCarree(),
    x='lon',y='lat',
    levels = 8
)
for a in ax:
    a.coastlines()
    fun.circle_for_polar_map(a)
    a.set_extent([0, 360, 40, 90], ccrs.PlateCarree())
    gl = a.gridlines(draw_labels=True)
    #a.add_feature(cy.feature.BORDERS)

ax[0].set_title('Historical q94 \n 2014-07-04')
ax[1].set_title('Historical q93 \n 2014-07-04')
ax[2].set_title('Historical q92 \n 2014-07-04')
ax[3].set_title('2020 product \n 2020-04-15')

gl.top_labels = False
gl.right_labels = False
plt.tight_layout()
plt.show()
```

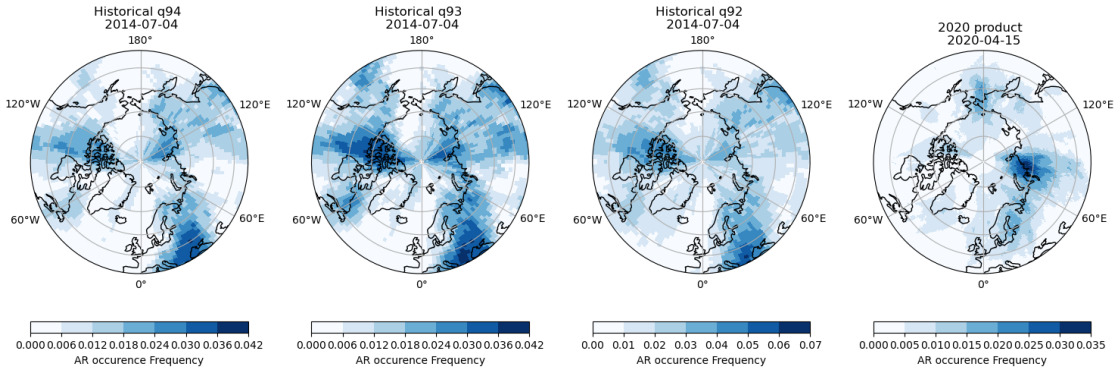

Figure S2: Average AR occurence plotted for 3 different IVT thresholds, and the 2020 detection product provided by Jonathan de Wille, using Wille et al., 2021, detection scheme on 3-hourly reanalysis data.

Figure S2 is also included for qualitative assesment rather than quantitative. What it shows is the spatial distribution of AR, and what we can see is again that there is a larger density in occurence close to the North pole with the q92 and q93 threshold. What is also worth noting in this figure is the pattern in AR distribution, it differs between our detection scheme and the one from Wille et al., 2021, but none of the detection schemes show a high frequency of AR occurance over the ocean between Scandinavia and Greenland. This is in direct contrast to Nash et al., 2018, who describe this region and the area between Alaska and Siberia as the main pathways for AR into the Arctic. Either this is another indication of the weaknesses of this detection, or it is in fact a strength, since it considers regionally high IVT. The water vapour concentration is higher over ocean than over land, so perhaps moisture transport is the highest in the pathways described by Nash et al., 2018, but aerosol transport by AR might be even more significant over land.